NATIONAL ADVISORY COMMITTEE FOR AERONAUTICS

REPORT No. 873

HIGH-ALTITUDE FLIGHT COOLING INVESTIGATION OF A RADIAL AIR-COOLED ENGINE

By EUGENE J. MANGANIELLO, MICHAEL F. VALERINO
and E. BARTON BELL

1947

For sale by the Superintendent of Documents, U. S. Government Printing Office, Washington 25, D. C. - - - - - Price 15 cents

AERONAUTIC SYMBOLS

1. FUNDAMENTAL AND DERIVED UNITS

	Symbol	Metric		English	
		Unit	Abbreviation	Unit	Abbreviation
Length	l	meter	m	foot (or mile)	ft (or mi)
Time	t	second	s	second (or hour)	sec (or hr)
Force	F	weight of 1 kilogram	kg	weight of 1 pound	lb
Power	P	horsepower (metric)		horsepower	hp
Speed	V	kilometers per hour	kph	miles per hour	mph
		meters per second	mps	feet per second	fps

2. GENERAL SYMBOLS

W Weight$=mg$

g Standard acceleration of gravity$=9.80665$ m/s^2 or 32.1740 ft/sec^2

m Mass$=\frac{W}{g}$

I Moment of inertia$=mk^2$. (Indicate axis of radius of gyration k by proper subscript.)

μ Coefficient of viscosity

ν Kinematic viscosity

ρ Density (mass per unit volume)

Standard density of dry air, 0.12497 kg-m^{-4}-s^2 at 15° C and 760 mm; or 0.002378 lb-ft^{-4} sec^2

Specific weight of "standard" air, 1.2255 kg/m^3 or 0.07651 lb/cu ft

3. AERODYNAMIC SYMBOLS

S Area

S_w Area of wing

G Gap

b Span

c Chord

A Aspect ratio, $\frac{b^2}{S}$

V True air speed

q Dynamic pressure, $\frac{1}{2}\rho V^2$

L Lift, absolute coefficient $C_L=\frac{L}{qS}$

D Drag, absolute coefficient $C_D=\frac{D}{qS}$

D_0 Profile drag, absolute coefficient $C_{D_0}=\frac{D_0}{qS}$

D_i Induced drag, absolute coefficient $C_{D_i}=\frac{D_i}{qS}$

D_p Parasite drag, absolute coefficient $C_{Dp}=\frac{D_p}{qS}$

C Cross-wind force, absolute coefficient $C_C=\frac{C}{qS}$

i_w Angle of setting of wings (relative to thrust line)

i_t Angle of stabilizer setting (relative to thrust line)

Q Resultant moment

Ω Resultant angular velocity

R Reynolds number, $\rho\frac{Vl}{\mu}$ where l is a linear dimension (e.g., for an airfoil of 1.0 ft chord, 100 mph, standard pressure at 15° C, the corresponding Reynolds number is 935,400; or for an airfoil of 1.0 m chord, 100 mps, the corresponding Reynolds number is 6,865,000)

α Angle of attack

ϵ Angle of downwash

α_0 Angle of attack, infinite aspect ratio

α_i Angle of attack, induced

α_a Angle of attack, absolute (measured from zero-lift position)

γ Flight-path angle

REPORT No. 873

HIGH-ALTITUDE FLIGHT COOLING INVESTIGATION OF A RADIAL AIR-COOLED ENGINE

By EUGENE J. MANGANIELLO, MICHAEL F. VALERINO
and E. BARTON BELL

Flight Propulsion Research Laboratory
Cleveland, Ohio

National Advisory Committee for Aeronautics

Headquarters, 1724 F Street NW, Washington 25, D. C.

Created by act of Congress approved March 3, 1915, for the supervision and direction of the scientific study of the problems of flight (U. S. Code, title 49, sec. 241). Its membership was increased to 15 by act approved March 2, 1929. The members are appointed by the President, and serve as such without compensation.

REPORT No. 873

HIGH-ALTITUDE FLIGHT COOLING INVESTIGATION OF A RADIAL AIR-COOLED ENGINE

By Eugene J. Manganiello, Michael F. Valerino and E. Barton Bell

SUMMARY

An investigation of the cooling of an 18-cylinder, twin-row, radial, air-cooled engine in a high-performance pursuit airplane has been conducted for variable engine and flight conditions at altitudes ranging from 5000 to 35,000 feet in order to provide a basis for predicting high-altitude cooling performance from sea-level or low-altitude experimental results.

The engine cooling data obtained were analyzed by the usual NACA cooling-correlation method wherein cylinder-head and cylinder-barrel temperatures are related to the pertinent engine and cooling-air variables. A theoretical analysis was made of the effect on engine cooling of the change of density of the cooling air across the engine (the compressibility effect), which becomes of increasing importance as altitude is increased. Good agreement was obtained between the results of the theoretical analysis and the experimental data. The use of the cooling-air exit density in the NACA cooling-correlation equation was found to be a sufficiently accurate approximation of the compressibility effect to give satisfactory correlation of the cooling data over the altitude range investigated. A sea-level or low-altitude correlation based on entrance density was also found to give fairly accurate cooling predictions up to an altitude of 20,000 feet.

INTRODUCTION

A method was developed at the NACA Langley laboratory (reference 1) for relating the cylinder-wall temperatures of an air-cooled engine with operating conditions, cooling-air temperature, and cooling-air weight flow. Because pressure drop is a more easily measurable quantity than weight flow and because the product of cooling-air entrance density (taken relative to standard sea-level air density) and pressure drop $\sigma_{en}\Delta p$ is a function of the weight flow, this product was substituted for weight flow in the correlation method. This substitution, which was made on the basis of incompressible-flow considerations, has proved satisfactory for the correlation of sea-level and low-altitude cooling data, as is evident from the results of numerous engine-cooling investigations (for example, references 2 and 3). For application to high-altitude flight, however, where the change of density of the cooling-air across the engine (compressibility effects) becomes significant, the weight flow and $\sigma_{en}\Delta p$ are not uniquely related and consequently the substitution is invalidated. Errors are therefore introduced in the prediction of high-altitude cooling from sea-level or low-altitude experimental results when the substitution is made.

Some theoretical and experimental investigations of the cooling problems at altitude have already been conducted. Reference 4 presents a theoretical study of the compressibility effect in relation to aircraft heat-exchanger operation and provides charts whereby, in a series of successive approximations, the compressible pressure drop corresponding to a given cooling-air weight flow, drag coefficient, and density change can be determined. A somewhat similar theoretical analysis of the compressibility effect in relation to engine cooling is given in reference 5, which provides charts for determining accurately compressible-flow cooling-air pressure drop. In addition, reference 5 indicates that the compressibility effect can be accounted for, to a good degree of accuracy, by the use of the product of pressure drop and exit density. This correlation of cooling-air weight flow with pressure drop on the basis of exit-density conditions was experimentally verified by Pratt & Whitney Aircraft in single-cylinder-engine experiments over a range of simulated altitudes from sea level to 45,000 feet. A similar single-cylinder investigation (reference 6) conducted and reported concurrently with the subject experiments further verifies experimentally and theoretically the use of exit density.

In order to obtain information on the cooling characteristics of air-cooled engines at altitude conditions and, in particular, to check present methods of extrapolating the data obtained from sea-level or low-altitude cooling experiments to high-altitude conditions, a flight cooling investigation was conducted on an 18-cylinder, twin-row, radial, air-cooled engine installed in a high-performance pursuit airplane. The investigation, which was conducted during 1943–44 at the NACA Cleveland laboratory, consisted of flights at variable engine and flight operating conditions at altitudes ranging from 5000 to 35,000 feet. The cooling data obtained were correlated by the NACA method developed in reference 1 as modified to account for cooling-air compressibility effects. A theoretical analysis was also made to check the validity of the use of cooling-air exit density in the correlation equation for approximating the compressibility effects.

INSTALLATION

Airplane and power plant.—The engine cooling experiments were conducted in a pursuit airplane on an 18-cylinder, twin-row, radial, air-cooled engine having a volumetric displacement of 2804 cubic inches. The compression ratio for

the engine is 6.65, the spark setting 20° B.T.C., and the valve overlap 40°. The engine is equipped with a single-stage, single-speed blower, which has an impeller diameter of 11 inches and a gear ratio of 7.6:1. A turbosupercharger consisting of a single-stage impulse turbine wheel with a 13.2-inch pitch-line diameter directly shafted to a 15-inch-diameter impeller provides the supercharging required for high-altitude operation. An injection-type carburetor meters the fuel to the engine at the inlet face of the engine-stage blower. The power plant is rated as follows:

Operating condition	Horsepower	Engine speed (rpm)	Altitude (ft)
Normal	1625	2550	29,000
Emergency maximum	2000	2700	27,000
Take-off	2000	2700	------

The engine power is delivered through a 2:1 reduction gear to an electrically controllable four-bladed propeller having a diameter of 12 feet, 2 inches. The propeller is fitted with shank cuffs and is not provided with a spinner hub.

A photograph of the airplane used in the flight investigation is presented in figure 1. A schematic diagram of the power-plant installation showing the general arrangement of the internal air-ducting system and the relative positions on the airplane of the engine, the cowling, the turbosupercharger, the intercooler, and the oil coolers is shown in figure 2. The engine cowling is of the NACA type C fitted with eight adjustable cowling flaps extending around the upper half of the cowling. A small fixed air gap between the engine cowling and the fuselage body extends around the lower half of the cowling to the auxiliary air-supply scoop. The opening of the auxiliary air-supply scoop, which supplies air to the carburetor, intercooler, oil coolers, and exhaust cooling shrouds, is located within the engine cowling at the bottom of the engine. The intercooler is mounted at the rear of the airplane slightly forward of the turbosupercharger and is provided with two separate cooling-air outlets and flaps, one on each side of the fuselage. The oil coolers are mounted in series with respect to the oil flow, one on each corner of the fuselage at the rear of the engine.

FIGURE 1.—Airplane used in engine-cooling flight investigation.

Engine cooling-air pressure measurements.—Although the experiments included an extensive cooling-air pressure survey in which a large number of pressure tubes and locations were used, only those tube combinations specified by recent NACA procedures as giving the best indication of the average cooling-air pressures ahead of and behind the engine were of interest. The tubes used for the average pressure indications and their locations are shown in figure 3.

The total pressure of the cooling air was measured ahead of the engine with open-end tubes H1, H2, H3, and H4 located on each front-row cylinder at the positions indicated in figure 3. These tubes were installed halfway between the fin tips and the cylinder baffle at a point about ⅛ inch behind the tangent point of the baffle-entrance curl. The cooling-air static pressure behind the engine was measured on each rear-row cylinder with open-end tube P3 installed in the stagnation region behind the cylinder top baffle and tubes P1 and P4 installed in the curl of the intake-side baffle. Care was taken in the installation of these tubes to insure that they received little if any velocity pressure.

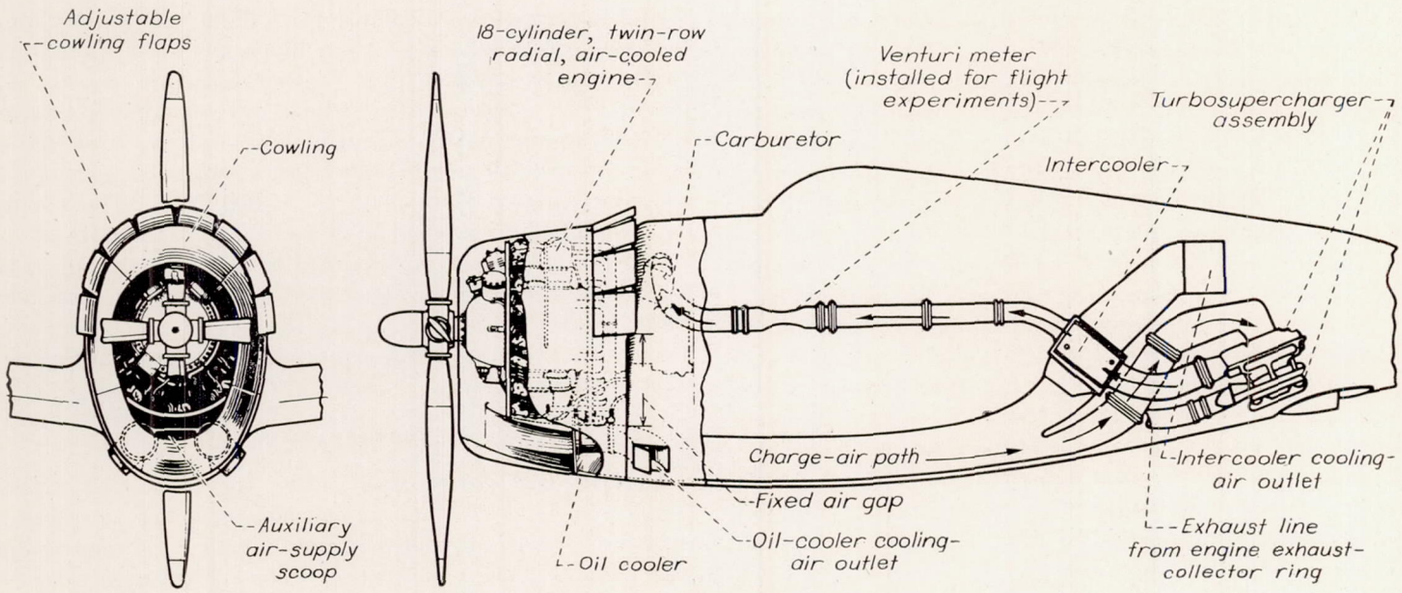

FIGURE 2.—Power-plant installation in airplane.

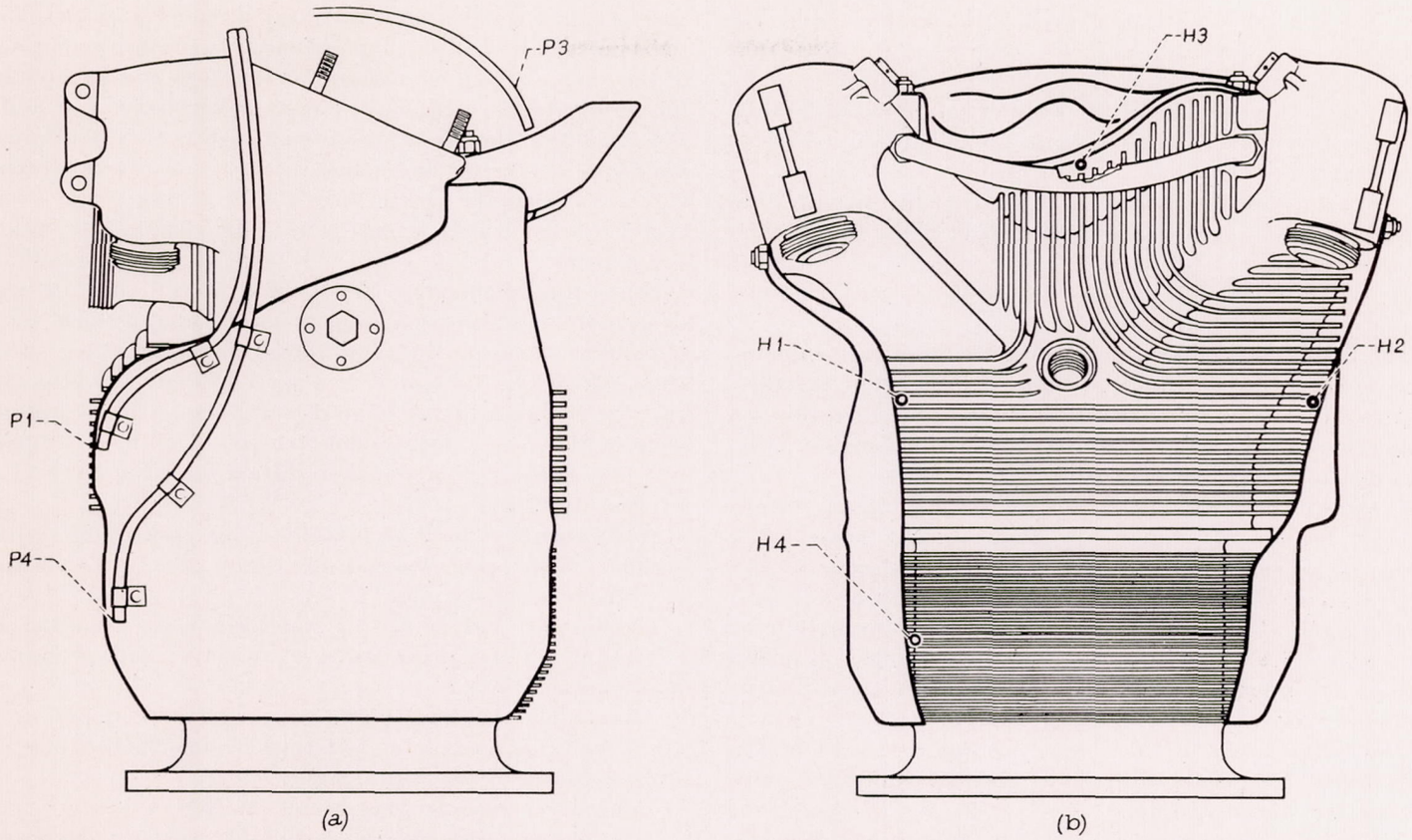

(a) Intake-side view of rear-row cylinder showing static-pressure tube locations.

(b) Front view of front-row cylinder showing total-pressure tube locations.

FIGURE 3.—Cylinder total- and static-pressure tube locations.

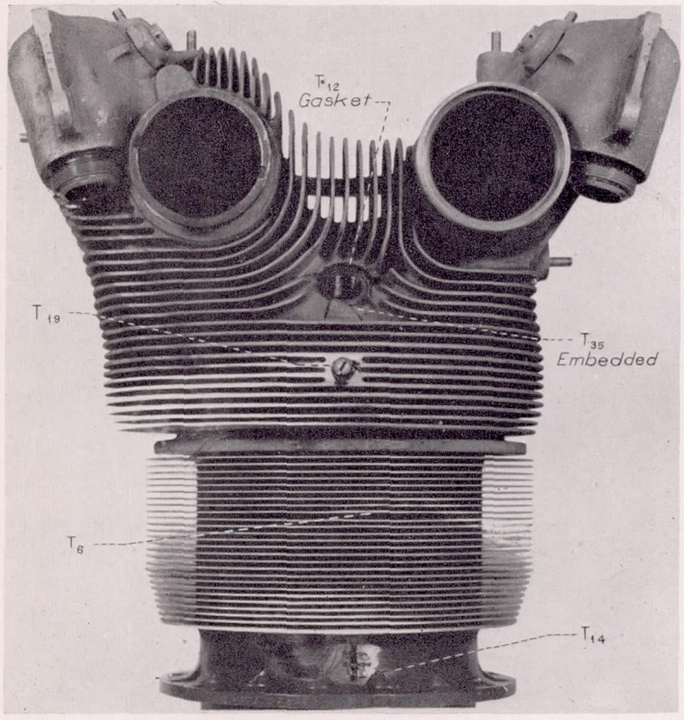

FIGURE 4.—Cylinder thermocouple locations.

The pressure tubes were led to motor-driven pressure-selector valves that, in turn, were connected to NACA recording multiple manometers. All pressures could be recorded in 2 minutes.

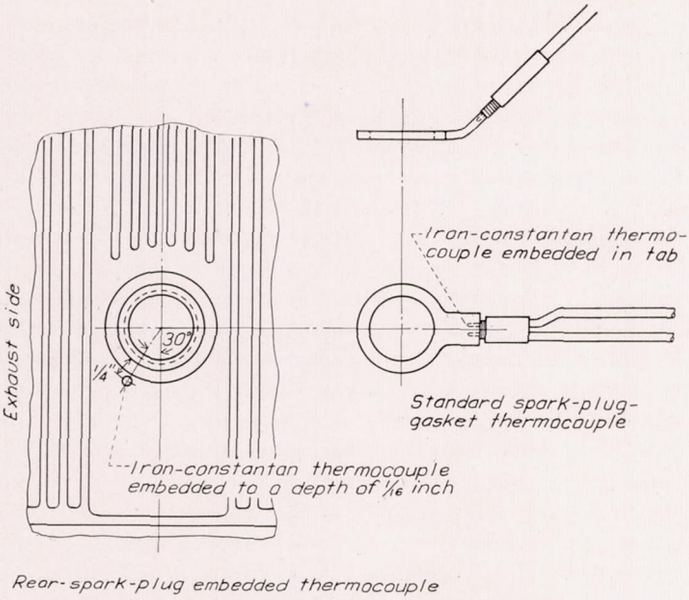

FIGURE 5.—Details of rear-spark-plug-boss and gasket thermocouples.

Temperature measurements.—Cylinder-wall temperatures were measured with iron-constantan thermocouples located on the heads and the barrels of each of the 18 engine cylinders. The locations and designations of these cylinder-wall thermocouples, which are indicated in figure 4, are:

(1) At the rear spark plug with standard gasket-type thermocouple T_{12}. (See fig. 5 for sketch of gasket-type-thermocouple details.)

(2) In the rear spark-plug boss with thermocouple T_{35} embedded to a depth of $\frac{1}{16}$ inch. (See fig. 5 for details of installation.)

(3) In the rear middle of the head circumferential finning with thermocouple T_{19} peened about $\frac{1}{16}$ inch into the cylinder-wall surface.

(4) In the rear of the barrel two-thirds of the way up with thermocouple T_6 peened about $\frac{1}{16}$ inch into the aluminum-barrel muff.

(5) At the rear of the cylinder base flange with thermocouple T_{14} spot-welded at the flange.

The free-air temperature was obtained from the temperature reading of a resistance-bulb thermometer installed under and near the tip of the right wing. The correction for stagnation-heating effect was determined in a separate flight calibration for various airspeeds.

A survey of the temperatures in the cooling-air stream directly behind the engine was made during most of the flight experiments. Eighteen iron-constantan thermocouples were used in this survey, two in front of each of the nine intake pipes at the same radial distances as the middle of the engine heads and barrels. The intake pipes provided partial shielding of the thermocouples from the exhaust-collector ring.

The temperature of the charge air was measured at the carburetor top deck with four parallel-connected iron-constantan thermocouples.

All temperatures were recorded by high-speed data recorders consisting of galvanometers, thermocouple selector switches, and film-drum recorders. It was possible to record 200 temperatures during each run in about 3 minutes. A calibration point was obtained for each galvanometer during each run by taking galvanometer readings of a known standard voltage; the effect of changing galvanometer calibration was thus eliminated. A check on the accuracy of the temperature records was also provided during each run by recording on each galvanometer the temperature of hot mercury contained within a thermos bottle.

Charge-air-weight-flow measurements.—The charge-air weight flow was measured during flight by venturi meters installed in the two parallel lines between the intercooler and the carburetor, as shown in figure 2, and calibrated within the charge-air ducting system prior to the flight experiments. In addition, checks were obtained from the carburetor compensated metering pressure as measured during flight and its relation with charge-air flow as established in extensive carburetor air-box experiments for the range of carburetor pressures and temperatures. The checks obtained were within ± 3 percent; the deviations were of a random nature.

Fuel-flow measurements.—A flow-bench calibration of the carburetor in which the fuel flow was related to the carburetor compensated metering pressure furnished the most direct and simplest method of measuring fuel flow in the flight experiments. This fuel-flow calibration was later verified in the air-box experiments, which showed the relation between compensated metering pressure and fuel flow to be independent of the pressure and temperature conditions of the charge air at the carburetor top deck and also of the fuel temperature, within the range encountered. In addition, fuel-flow checks were obtained with both a deflecting-vane-type flowmeter and a fuel rotameter in several special flights covering the engine fuel-flow operating range. Except for a few widely erratic points, the checks were within ± 3 percent.

Other measurements.—Free-stream impact pressure was measured by a shrouded total-pressure tube installed on a streamline boom on the right wing tip. A swiveling static tube, which was calibrated in a special flight, was also carried by the boom about 1 chord length ahead of the leading edge of the wing. Continuous records of both the impact and static pressures were taken during each run by NACA pressure recorders.

A torquemeter was incorporated for measuring engine torque. The torque was indicated on a gage in the cockpit and was read by the pilot.

Engine and turbine speeds were separately recorded by revolution counters operated in conjunction with a chronometric timer.

The engine exhaust pressure was measured by means of static wall taps located on both sides of the exhaust collector ring upstream of the waste gate.

Continuous records were taken on NACA pressure and control-position recorders of manifold pressure; charge-air pressure at the turbosupercharger outlet and at the carburetor top deck; throttle setting; mixture-control setting; angle of attack; and engine, oil cooler, and intercooler flap openings.

PROCEDURE

The flight investigation was conducted, for the most part, at altitudes (based on pressure) of 5000, 25,000, 30,000, and 35,000 feet; a few flights were also made at intermediate altitudes. The three main controllable variables during each run at a given altitude were engine power, engine speed, and engine cooling-air pressure drop; in general, during each constant-altitude flight one of these three variables was independently varied while the other two were maintained constant.

The engine power was controlled with the carburetor throttle at constant engine speed and, at the high altitudes, also with the exhaust waste gate through regulation of the turbosupercharger speed. The mixture control was set in the automatic-rich position and the fuel-air ratio was allowed to vary according to the carburetor characteristics. The engine speed was controlled with the propeller governor and the cooling-air pressure drop was controlled by means of cowling-flap deflection and through change in the airplane drag characteristics (and thus the airplane velocity and available ram pressure) obtained by raising and lowering the landing gear.

A summary of the flight conditions is presented in table I. During each run, in which the specified conditions were held constant and the cylinder-wall temperatures had been stabilized, a record was obtained of the cooling-air pressures and temperatures ahead of and behind the engine, the cylinder-wall temperatures, and the airplane engine operating conditions.

REDUCTION OF COOLING DATA

Correlation equations.—The basic equation developed in reference 1 for correlating the wall temperatures of air-cooled engines with the engine operating conditions and the cooling-air temperature and weight flow is

$$\frac{\frac{T_h-T_a}{T_g-T_h}}{W_c^n}=\frac{K_1}{W_a^r} \tag{1}$$

(All symbols are defined in appendix A.)

It has been the practice in low-altitude cooling-correlation work to assume that the cooling-air weight flow W_a is a function of the more readily measured quantity $\sigma_{en}\Delta p$ and to make this substitution in equation (1). The assumption that W_a is a unique function of $\sigma_{en}\Delta p$ has, however, been shown to be inaccurate for large altitude changes by various theoretical analyses (references 4, 5, and 6) and some experimental data.

In appendix B, which presents a theoretical treatment of the relation between cooling-air weight flow and pressure drop, W_a is shown to be more correctly a function of σ_{ex}/σ_{en} in addition to $\sigma_{en}\Delta p$. On the basis of the results of appendix B, equation (1) is written

$$\frac{\frac{T_h-T_a}{T_g-T_h}}{W_c^n}=\frac{K_2}{(\sigma_{en}\Delta p)^m}\,\phi\left(\frac{\sigma_{ex}}{\sigma_{en}}\right) \tag{2}$$

where $\phi(\sigma_{ex}/\sigma_{en})$ denotes a function of σ_{ex}/σ_{en}.

At low altitudes, the variation of σ_{ex}/σ_{en} over the normal engine operating range is sufficiently small that its function may be considered as a constant, with negligible sacrifice in accuracy. For substantially constant σ_{ex}/σ_{en}, equation (2) becomes the familiar correlation equation

$$\frac{\frac{T_h-T_a}{T_g-T_h}}{W_c^n}=\frac{K_3}{(\sigma_{en}\Delta p)^m} \tag{2a}$$

When a large altitude range is considered, in which case large variations in σ_{ex}/σ_{en} are encountered, the variations of the function $\phi(\sigma_{ex}/\sigma_{en})$ must be included in equation (2) In appendix B, $\phi(\sigma_{ex}/\sigma_{en})$ is theoretically derived. If it is assumed that

$$\phi\left(\frac{\sigma_{ex}}{\sigma_{en}}\right)=K_4\left(\frac{\sigma_{ex}}{\sigma_{en}}\right)^{-b}$$

equation (2) reduces to

$$\frac{\frac{T_h-T_a}{T_g-T_h}}{W_c^n}=\frac{K}{(\sigma_{en}\Delta p)^m\left(\frac{\sigma_{ex}}{\sigma_{en}}\right)^b} \tag{3}$$

The constants n, m, b, and K will be evaluated from the experimental data.

In order for exit density (as suggested in reference 5 and as theoretically shown in reference 6) to be a satisfactory basis of correlation, it is necessary that $b=m$ in equation (3), in which case equation (3) reduces to

$$\frac{\frac{T_h-T_a}{T_g-T_h}}{W_c^n}=\frac{K}{(\sigma_{ex}\Delta p)^m} \tag{4}$$

The accuracy of the foregoing simplification will be empirically checked with the flight data. Equations similar to equations (1) to (4) may also be written for the engine barrels.

Some investigators (for example, reference 7) believe that, in order to obtain accurate correlation, the local cooling-air temperature in the vicinity of the spot on the cylinder wall under investigation (at the location where T_h is measured) should be used instead of the entrance cooling-air temperature. In appendix C, it is shown that the cooling-correlation equation containing the local cooling-air temperature can be transposed to the equation containing entrance cooling-air temperature; hence either temperature can be used. The inlet cooling-air temperature was used in the correlation presented herein because the added complication of determining the local cooling-air temperature did not appear warranted.

Mean effective gas temperature T_g.—The mean effective gas temperature T_g is, for a given engine, considered a function of fuel-air ratio, inlet-manifold temperature, exhaust pressure, and spark timing.

On the basis of previous correlation work, a $T_{g,80}$ value of 1150° F for the heads and 600° F for the barrels is chosen for the reference conditions of $F/A=0.08$, $T_m=80°$ F, and $p_e=30$ inches of mercury absolute, and for the normal spark setting.

The variation of $T_{g,80}$ with fuel-air ratio for the sea-level exhaust-pressure condition (approximately 30 in. Hg absolute) is taken as that determined in previous cooling experiments on an R–2800–21 single-cylinder engine (reference 8). This $T_{g,80}$ variation, which was also found to check well with the results obtained on other types and models of air-cooled engine, is plotted for the heads and barrels in figure 6. The variation of $T_{g,80}$ with exhaust pressure for the range covered

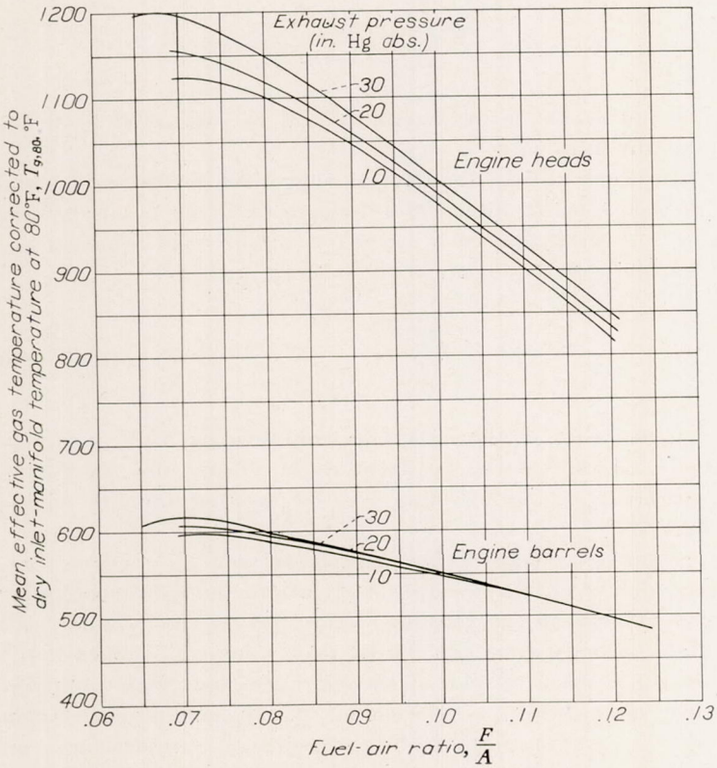

FIGURE 6.—Variation of mean effective gas temperature corrected to dry inlet-manifold temperature at 80° F. with fuel-air ratio and exhaust pressure.

in the present investigation is included in figure 6 and represents the results of extensive exhaust-pressure experiments conducted at the Cleveland laboratory on an R–2800–5 engine. Inasmuch as the engine normal spark timing was used throughout the investigation, the effect of this variable is not required for analysis of the cooling data.

The correction applied to $T_{g,80}$ to obtain T_g for values of T_m other than 80° F is given as $\Delta T_g=0.8\ (T_m-80)$ for engine heads and $\Delta T_g=0.5\ (T_m-80)$ for engine barrels. The dry inlet-manifold temperature T_m is calculated from the carburetor inlet-air temperature and the theoretical blower temperature rise, assuming no fuel vaporization. This relation is given as

$$T_m=T_c+\frac{U^2}{gJc_p} \tag{5}$$

For the engine used in the present investigation, equation (5) reduces to

$$T_m=T_c+22.1\left(\frac{N}{1000}\right)^2 \tag{6}$$

Cylinder temperatures.—The value of cylinder-head temperature T_h used in the primary correlation is taken as the average for the 18 cylinders of the temperature indications of the thermocouples peened into the rear middle of the heads (T_{19} in fig. 4); the barrel temperature T_b is taken as the average of the temperature indications of the thermocouples peened into the rear of the barrels (T_6 in fig. 4). Final correlation curves based on the rear-spark-plug-gasket and boss-embedded-thermocouple readings (T_{12} and T_{35} in fig. 4) are also presented to permit cooling comparisons with the results of other investigations.

Cooling-air temperatures.—The entrance cooling-air temperature T_a is taken as the stagnation air temperature ahead of the engine as calculated from the free-air temperature and the airplane velocity measurements.

The exit cooling-air temperature, which is required for calculation of the exit density, was obtained for about 90 percent of the experiments from the average of the temperature indications of the thermocouples located in the cooling-air stream behind the engine, the values for the engine-head and engine-barrel cooling air being separately averaged. These data were correlated by means of a relation developed in appendix D, which results in a single curve involving the cooling-air pressure drop and the ratio of the temperature rise of the cooling air ΔT to the temperature difference between the cylinder head and the entrance cooling air T_h-T_a. In the correlation of the cooling data, the exit cooling-air temperatures for all the experiments are calculated from this curve.

Cooling-air pressure drop and density.—The average cooling-air pressure drops across the engine heads and barrels are separately determined as the difference between the average total pressure ahead of and the average static pressure behind the engine heads or barrels.

The average for the front-row cylinders of the readings of the tubes designated H1, H2, and H3 (fig. 3) is taken as the average pressure in front of the engine heads; the average of the readings of the tubes H4 is taken as the average pressure in front of the engine barrels.

The average static pressure behind the engine heads is obtained from the average for the rear-row cylinders of the readings of tubes P1 and P3; tubes P4 are used for obtaining the average static pressure behind the engine barrels.

The entrance density of the cooling air is calculated from the stagnation-air temperature and the total-pressure values ahead of the engine; conversion into entrance density ratio σ_{en} is made simply by dividing by the standard sea-level density value (0.0765 lb/cu ft). The exit density of the cooling air is calculated from the exit-air-temperature and static-pressure values behind the engine and is converted into exit density ratio σ_{ex} by dividing by standard sea-level density.

Although the exit density is readily calculated from the measurements of temperature and pressure made in the flight investigation, its evaluation for use in predicting cooling performance from an established correlation is indirect inasmuch as it involves a knowledge of the temperature rise and pressure drop of the cooling air across the engine. A method of calculating the exit density for use in cooling predictions is given in appendix E.

Constants m, n, and K_3.—The exponents m and n of $\sigma_{en}\Delta p$ and W_c, respectively, and the constant K_3 are determined from the cooling data obtained at a constant σ_{ex}/σ_{en} (for all practical purposes, at a constant altitude) by means of the familiar correlation procedure expressed in equation (2a).

The function ϕ $(\sigma_{ex}/\sigma_{en})$.—In order to check the validity of the theoretically derived equations (3) and (4), the function $\phi(\sigma_{ex}/\sigma_{en})$, which represents the effect of cooling-air compressibility in the generalized correlation equation (equation (2)), is experimentally determined by plotting $\frac{T_h-T_a}{T_g-T_h}\frac{(\sigma_{en}\Delta p)^m}{W_c^n}$ against σ_{ex}/σ_{en} from the data obtained at different altitudes. In order to minimize the extraneous effects resulting from differences in engine operating conditions that may not correlate accurately and may therefore mask the less sensitive effects of the cooling-air density change, data are selected, in the construction of this plot, for a narrow range of engine operating conditions (1200 and 1500 bhp; engine speed, 2550 rpm; fuel-air ratio, 0.12). In addition, in order to increase the over-all accuracy of the plotted parameters through reduction of the random percentage errors associated with the experiments, the values of the parameters for the individual runs of each variable cooling-air pressure flight (five to six runs per flight) are averaged to give one plotted point per flight.

RESULTS AND DISCUSSION

Determination of constants m, n, and K_3.—The determination of the exponent m on $\sigma_{en}\Delta p$ (equation (2)) is shown in figure 7 where plots of $\frac{T_h-T_a}{T_g-T_h}$ and $\frac{T_b-T_a}{T_g-T_b}$ against $\sigma_{en}\Delta p$ are made from the data obtained at an approximately constant σ_{ex}/σ_{en} value of 0.83 (constant altitude of 5000 ft) in flights that were each conducted at substantially constant charge-air weight flow, fuel-air ratio, and engine speed with variable cooling-air pressure drop. Lines with the best-fitting constant slope are drawn through the plotted values for each of the flights. The common slope, which is the negative value of m in equation (2), is -0.35 for the engine heads and -0.43 for the engine barrels.

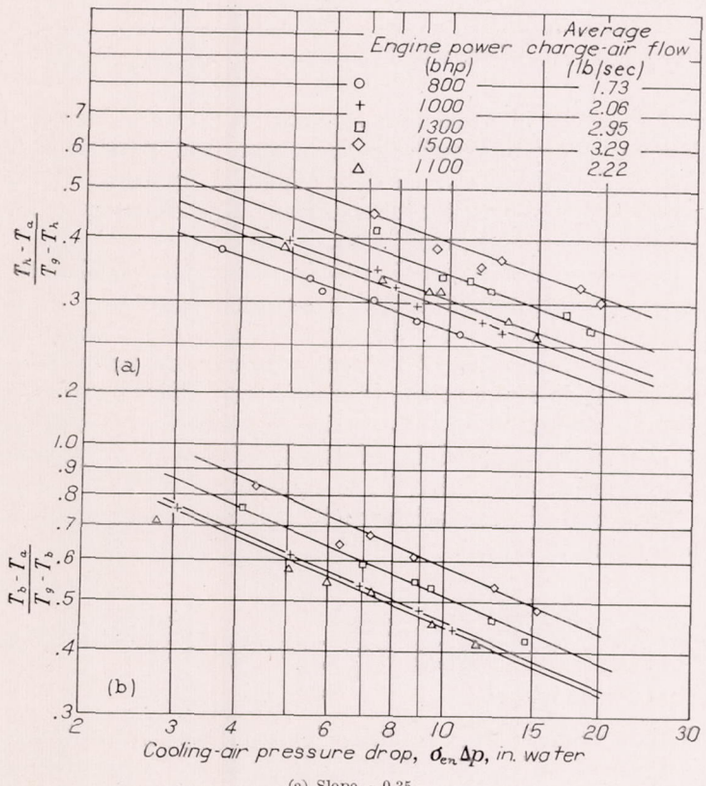

(a) Slope, −0.35.
(b) Slope, −0.43.

FIGURE 7.—Variation of $\frac{T_h-T_a}{T_g-T_h}$ and $\frac{T_b-T_a}{T_g-T_b}$ with cooling-air pressure drop $\sigma_{en}\Delta p$ for various constant charge-air flows at altitude of 5000 feet ($\sigma_{ex}/\sigma_{en}=0.83$).

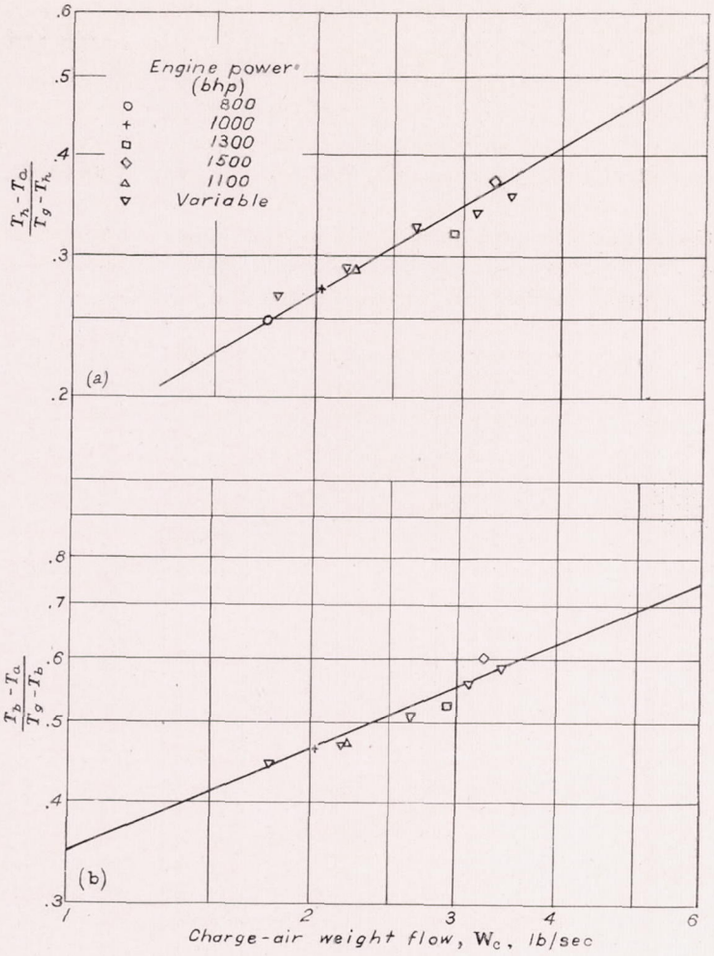

(a) Slope, 0.60.
(b) Slope, 0.43.

FIGURE 8.—Variation of $\frac{T_h-T_a}{T_g-T_h}$ and $\frac{T_b-T_a}{T_g-T_b}$ with charge-air weight flow W_c at constant cooling-air pressure drop of 12 and 9 inches of water for heads and barrels, respectively, at altitude of 5090 feet ($\sigma_{ex}/\sigma_{en}=0.83$). (Cross plot of fig. 7.)

A cross plot from figure 7 of the values of $\frac{T_h-T_a}{T_g-T_h}$ and $\frac{T_b-T_a}{T_g-T_b}$ against charge-air weight flow W_c for a constant $\sigma_{en}\Delta p$ value of 12 inches of water for the heads and 9 inches of water for the barrels is presented in figure 8. Included in this figure are the cooling results obtained in a single flight conducted for variable charge-air weight flow at an approximately constant σ_{ex}/σ_{en} value of 0.83 and $\sigma_{en}\Delta p$ values of 12 and 9 inches of water for the heads and the barrels, respectively. The plotted values for the variable charge-air-flow flight

fall in with the points taken from the cross plot of figure 7. These points determine a slope of 0.60 for the heads and 0.43 for the barrels, which are the respective values of n (equation (2)) for the engine heads and barrels.

The values of $\frac{T_h-T_a}{T_g-T_h}\Big/W_c^{0.60}$ and $\frac{T_b-T_a}{T_g-T_b}\Big/W_c^{0.43}$, as calculated from the data obtained in all the flights conducted at σ_{ex}/σ_{en} of approximately 0.83 (altitude, 5000 ft), are plotted in figure 9 against the corresponding $\sigma_{en}\Delta p$ values. A line

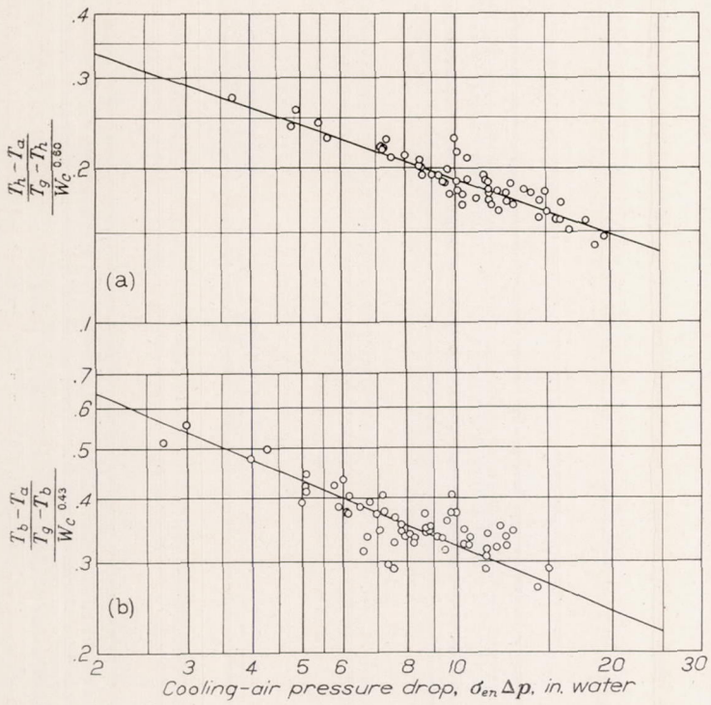

(a) Slope, −0.35.
(b) Slope, −0.43.

FIGURE 9.—Cooling-correlation curves based on entrance density for engine heads and barrels at altitude of 5000 feet.

with the previously determined slope $-m$ (−0.35 for the heads and −0.43 for the barrels) is drawn to best represent the plotted values. The correlation equation, which represents the correlation line drawn in figure 9 for σ_{ex}/σ_{en} of 0.83, is expressed for the engine heads as

$$\frac{\frac{T_h-T_a}{T_g-T_h}}{W_c^{0.60}}=\frac{0.42}{(\sigma_{en}\Delta p)^{0.35}} \tag{7}$$

and the engine barrels as

$$\frac{\frac{T_b-T_a}{T_g-T_b}}{W_c^{0.43}}=\frac{0.85}{(\sigma_{en}\Delta p)^{0.43}} \tag{8}$$

The constants of 0.42 in equation (7) and 0.85 in equation (8) are equal to $K_2\ \phi\ (\sigma_{ex}/\sigma_{en})$ in the general correlation expression (equation (2)) and to K_3 in equation (2a).

Determination of function ϕ $(\sigma_{ex}/\sigma_{en})$.—In accordance with equation (2), the values of $\left(\frac{T_h-T_a}{T_g-T_h}\Big/W_c^{0.60}\right)[(\sigma_{en}\Delta p)^{0.35}]$, averaged for each flight at constant engine conditions but variable cooling-air pressure drop, are plotted in figure 10

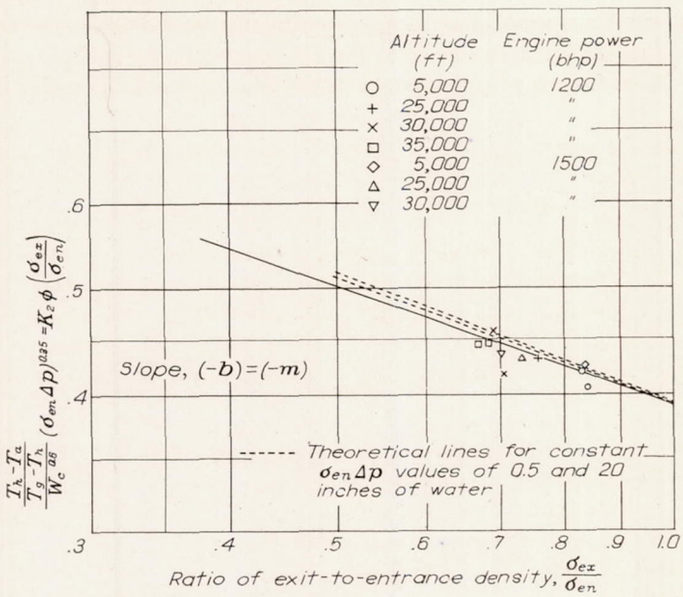

FIGURE 10.—Experimental variation of compressibility function $\phi\left(\frac{\sigma_{ex}}{\sigma_{en}}\right)$ with σ_{ex}/σ_{en} and comparison with theoretically determined variation.

against the corresponding σ_{ex}/σ_{en} values. The plotted points define a variation of increasing $\phi\ (\sigma_{ex}/\sigma_{en})$ with decreasing σ_{ex}/σ_{en} thus indicating the detrimental effect of cooling-air compressibility on engine cooling. This effect is the well-known altitude effect, which, for constant $\frac{T_h-T_a}{T_g-T_h}\Big/W_c^n$ is reflected as an increase $\sigma_{en}\Delta p$ requirement with increased altitude. Curves describing the theoretical variations of $\phi\ (\sigma_{ex}/\sigma_{en})$ with σ_{ex}/σ_{en}, as determined in appendix B, are included in figure 10 for comparison. Agreement with the experimental results is indicated.

The exponent b in equation (3) is numerically equal to the slope of a straight line through the points in figure 10. A line having a slope of −0.35 (the negative value of the exponent m of $\sigma_{en}\Delta p$ in equation (7)) is drawn through the point representing the data at an altitude of 5000 feet. This line gives a good representation of the experimental data and also of the theoretical curves and is arbitrarily chosen as it permits simplification of equation (3) to equation (4).

The correlation equation for the cylinder heads obtained from figure 10 is

$$\frac{\frac{T_h-T_a}{T_g-T_h}}{W_c^{0.60}}=\frac{0.39}{(\sigma_{en}\Delta p)^{0.35}\left(\frac{\sigma_{ex}}{\sigma_{en}}\right)^{0.35}}=\frac{0.39}{(\sigma_{ex}\Delta p)^{0.35}} \tag{9}$$

The constant of 0.39 in equation (9) is the experimental value of K in equation (4). When σ_{ex}/σ_{en} is set equal to 0.83 (value for experiments at an altitude of 5000 ft), equation (9) reduces to equation (7).

Attempts to determine the function $\phi\ (\sigma_{ex}/\sigma_{en})$ for the cylinder barrels by the foregoing method were unsuccessful because of the large scatter of data, which masked the effect

of the function $\phi\ (\sigma_{ex}/\sigma_{en})$ on the barrel cooling. In the correlation of the barrel data presented in the subsequent section, however, the function $\phi\ (\sigma_{ex}/\sigma_{en})$ for the barrels is assumed to be similar to that for the heads and the exponent b is equal to the value of m for the barrels (0.43).

Correlation of all data on basis of $\sigma_{ex}\Delta p$.—The values of

$$\frac{T_h-T_a}{T_g-T_h}\Big/W_c^{0.60} \quad \text{and} \quad \frac{T_b-T_a}{T_g-T_b}\Big/W_c^{0.43}$$

calculated from the data obtained in all the flight experiments covering a range of altitudes from 5000 to 35,000 feet (equivalent to a range of σ_{ex}/σ_{en} from 0.83 to 0.62) are plotted in figure 11 against the corresponding $\sigma_{ex}\Delta p$ values. The correlation line given by equation (9) for the engine heads is indicated in figure 11. This single correlation line well represents both the low-

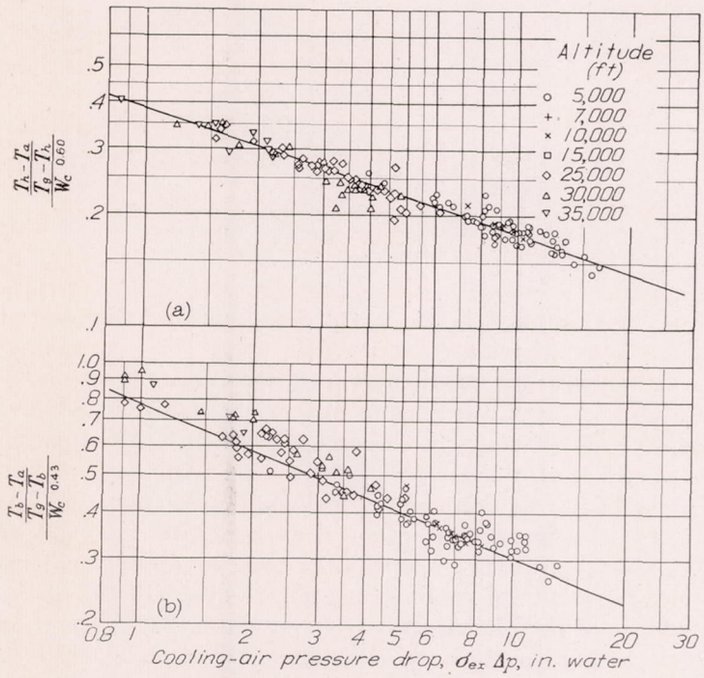

(a) Slope, −0.35; line given by equation (9) as determined for variable σ_{ex}/σ_{en}.
(b) Best-fitting line with predetermined slope of −0.43.

FIGURE 11.—Cooling-correlation curves based on exit density for engine heads and barrels for altitudes from 5000 to 35,000 feet.

altitude and the high-altitude cooling data. The best line with the previously determined slope of −0.43 is drawn through the plotted values for the barrel. For the data on the barrel, the agreement between the plotted values and the line is only fair at the high-altitude conditions but no definite conclusions can be drawn because of the large data scatter. The equation that describes this line is

$$\frac{T_b-T_a}{T_g-T_b}\Big/W_c^{0.43}=\frac{0.77}{(\sigma_{ex}\Delta p)^{0.43}} \tag{10}$$

Correlation of all data on basis of $\sigma_{en}\Delta p$.—The variable-altitude cooling data are plotted against $\sigma_{en}\Delta p$ in figure 12 wherein comparison is made with the correlation line given for σ_{ex}/σ_{en} equal to 0.83 (5000-ft altitude) by equations (7) and (8) for the engine heads and barrels, respectively. Because of the experimental variation of σ_{ex}/σ_{en}, which is not accounted for by the correlation line, the data points obtained at the high altitudes, although quite scattered, tend to fall slightly above the correlation line and show a definite trend of increasing deviation with increase in altitude. This general grouping of the high-altitude data points above the 5000-foot correlation line again indicates a greater $\sigma_{en}\Delta p$ requirement at the higher altitudes. Even for as high an altitude as 35,000 feet, however, the deviations are only of the same order as the spread in the data points.

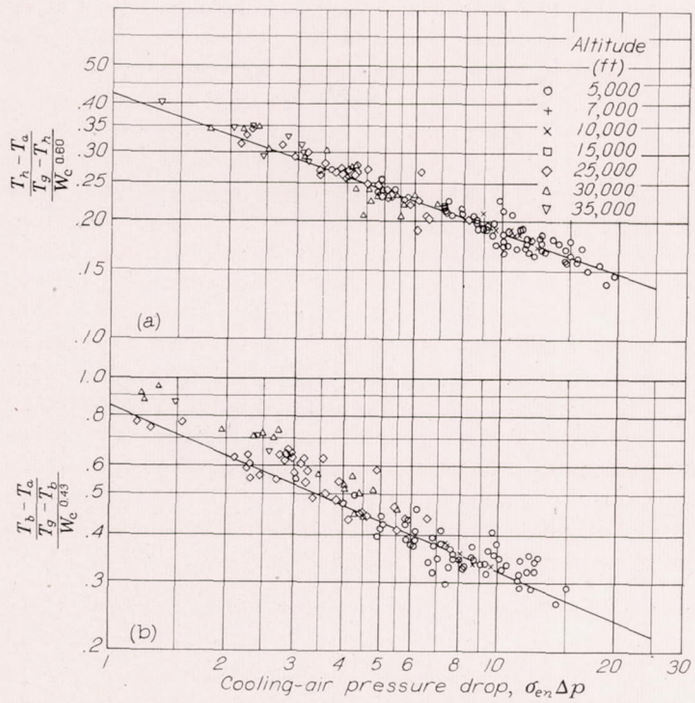

(a) Slope, −0.35; line as given by equation (7) for $\sigma_{ex}/\sigma_{en}=0.83$ (5000-ft correlation line).
(b) Slope, −0.43; line as given by equation (8) for $\sigma_{ex}/\sigma_{en}=0.83$ (5000-ft correlation line).

FIGURE 12.—Cooling-correlation curves based on entrance density for engine heads and barrels for altitudes from 5000 to 35,000 feet.

An examination of the plotted points in figure 12 indicates that a single line with a slightly higher slope than the correlation line for constant σ_{ex}/σ_{en} can be drawn to fit satisfactorily all the data. This apparent data correlation can be explained with reference to figure 13, which presents, for the

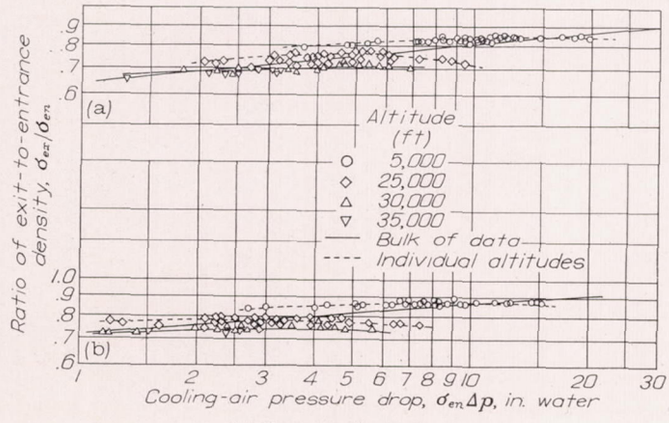

(a) Slope, s; engine heads.
(b) Slope, s; engine barrels.

FIGURE 13.—Variation of σ_{ex}/σ_{en} with cooling-air pressure drop $\sigma_{en}\Delta p$ at altitudes from 5000 to 35,000 feet for engine heads and barrels.

same data as in figure 12, a plot of σ_{ex}/σ_{en} against $\sigma_{en}\Delta p$ on logarithmic coordinate paper. Although the relation between σ_{ex}/σ_{en} and $\sigma_{en}\Delta p$ is actually different for the different altitudes, the bulk of the data for the entire altitude experimental range can be roughly represented by a single relation expressed as $\sigma_{ex}/\sigma_{en}=K_5(\sigma_{en}\Delta p)^s$. The use of a single relation is made possible in this case only because of the operational limitations of the engine-airplane combination that causes a shift in operating range of $\sigma_{en}\Delta p$ with altitude; for example, at an altitude of 5000 feet (σ_{ex}/σ_{en}=approximately 0.83), a range of $\sigma_{en}\Delta p$ of approximately 4 to 20 inches of water was covered in the experiments; whereas at an altitude of 30,000 feet (σ_{ex}/σ_{en}=approximately 0.75), the $\sigma_{en}\Delta p$ range is approximately 1.5 to 5.5 inches of water. Substitution of $K_5(\sigma_{en}\Delta p)^s$ for σ_{ex}/σ_{en} and the value of m for b in equation (3) reduces the right-hand term of this equation to $K_6/(\sigma_{en}\Delta p)^{m(1+s)}$, which gives $m(1+s)$ as the slope of the line best correlating the plotted points in figure 12. Inasmuch as the establishment of this correlation is dependent on the variation obtained in the experiments of σ_{ex}/σ_{en} with $\sigma_{en}\Delta p$, it is applicable for use in predictions only when the operating conditions satisfy the experimental relation between σ_{ex}/σ_{en} and $\sigma_{en}\Delta p$. This correlation is therefore of no reliable aid in altitude and pressure-drop extrapolations.

Correlation of average rear-spark-plug-boss and gasket temperatures.—Inasmuch as the cooling of aircraft engines is frequently evaluated on the basis of the rear-spark-plug-boss and gasket temperatures, the correlation results based on these temperature readings (T_{35} and T_{12} in fig. 4) are presented in figures 14 and 15 as plots of $\dfrac{T_{35}-T_a}{T_g-T_{35}}\Big/W_c^{0.60}$ and $\dfrac{T_{12}-T_a}{T_g-T_{12}}\Big/W_c^{0.60}$, respectively, against $\sigma_{ex}\Delta p$ and $\sigma_{en}\Delta p$. As an indication of the accuracy of the general experimental results, the correlation line for the rear-spark-plug-boss temperature checks within an average accuracy of 10° F

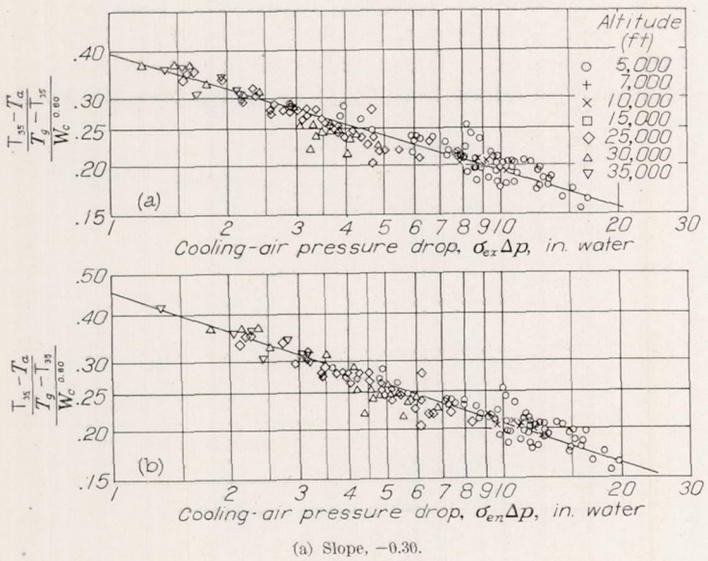

(a) Slope, −0.30.
(b) Slope, −0.34.

FIGURE 14.—Cooling-correlation curves based on rear-spark-plug-boss embedded thermocouples for exit and entrance density for altitudes from 5000 to 35,000 feet. (Curves drawn to best fit all data.)

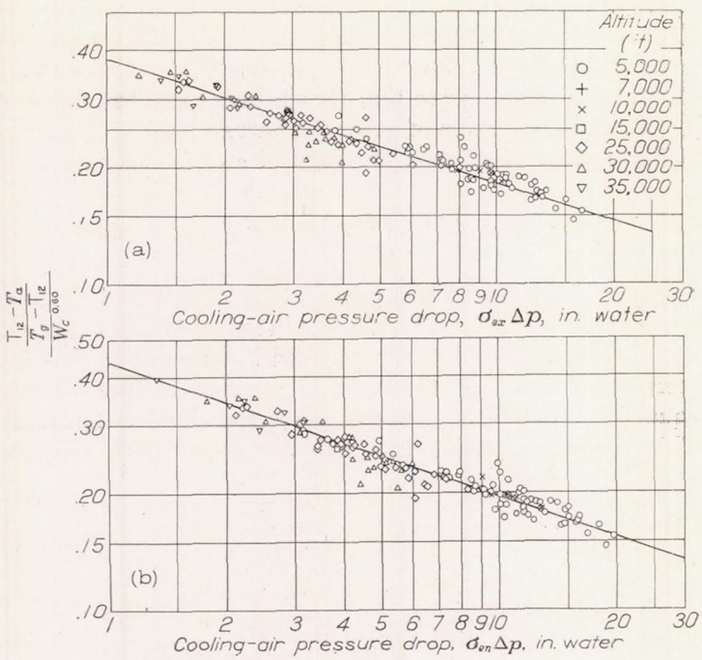

(a) Slope, −0.32.
(b) Slope, −0.35.

FIGURE 15.—Cooling-correlation curves based on rear-spark-plug-gasket thermocouples for exit and entrance density for altitudes from 5,000 to 35,000 feet. (Curves drawn to best fit all data.)

with that obtained in an NACA test-stand investigation of a similar multicylinder engine.

Altitude-cooling predictions from sea-level correlation.—A comparison of the cooling obtained at altitude, as predicted by the cooling-correlation line based on $\sigma_{ex}\Delta p$ (equation (9)) with that indicated by the sea-level cooling-correlation (actually 5000-ft altitude) line based on $\sigma_{en}\Delta p$ (equation (7)) is shown in figure 16 as a plot of average head temperature T_{19} against altitude for constant engine conditions and two constant values of cooling-air pressure drop (10 and 20 in. water). The difference between the curve based on $\sigma_{ex}\Delta p$ and that based on $\sigma_{en}\Delta p$ amounts to 9° F at 20,000 feet, 13° F at 30,000 feet, and 36° F at 50,000 feet, when the

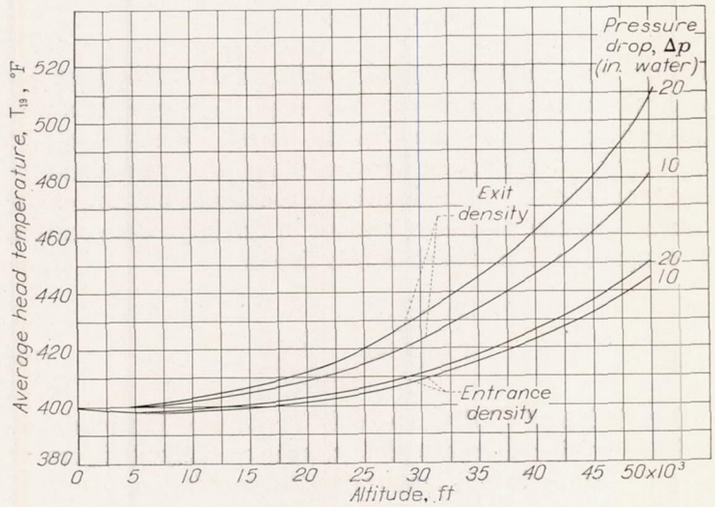

FIGURE 16.—Calculated variation in average head temperature with altitude based on both entrance and exit density for pressure drops of 10 and 20 inches of water. Engine power, 1625 brake horsepower; engine speed, 2400 rpm; charge-air weight flow, 3.5 pounds per second; Army summer air.

cooling-air pressure drop is 10 inches of water. For a cooling-air pressure drop of 20 inches of water, differences of 9°, 20°, and 60° F are obtained for 20,000, 30,000, and 50,000 feet, respectively.

The magnitude of the errors introduced when predicting high-altitude pressure-drop requirements from the low-altitude correlation line based on $\sigma_{en}\Delta p$ rather than $\sigma_{ex}\Delta p$ is illustrated in figure 17, which presents, for a given set of

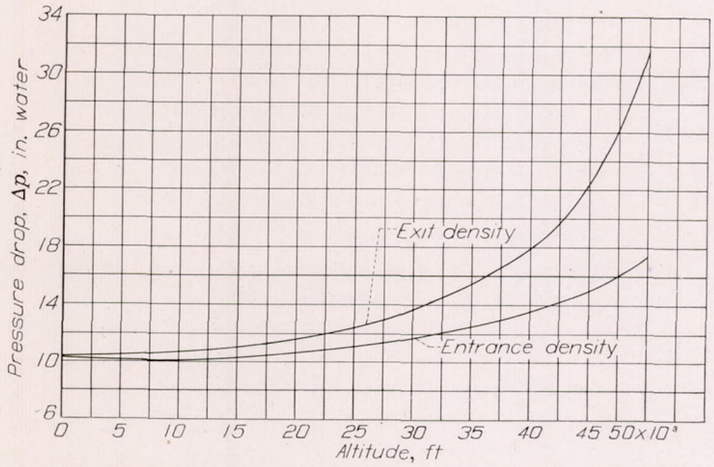

FIGURE 17.—Calculated variation of pressure drop with altitude necessary to maintain constant head temperature T_{19}. Engine power, 1625 brake horsepower; engine speed, 2400 rpm; charge-air weight flow, 3.5 pounds per second; fuel-air ratio, 0.10; Army summer air.

constant engine operating conditions, the cooling-air pressure-drop variation with altitude as calculated by both correlations for maintaining an average head temperature of 400° F. Errors in cooling-air pressure drop of 1, 2, and 14 inches of water are indicated for 20,000, 30,000, and 50,000 feet, respectively.

Altitude predictions from a sea-level correlation based on $\sigma_{en}\Delta p$ are fairly accurate up to 20,000 feet, as shown in figures 16 and 17, but the error increases so rapidly with further increase in altitude that the correlation based on $\sigma_{ex}\Delta p$ should be used at the higher altitudes.

SUMMARY OF RESULTS

The results of an engine cooling flight investigation conducted on an 18-cylinder, twin-row, radial, air-cooled engine in a pursuit airplane for a range of altitudes from 5000 to 35,000 feet showed that:

1. The effect of cooling-air compressibility on the cooling characteristics of air-cooled engines was accounted for, to a good degree of accuracy, by the use in the NACA cooling-correlation method of the cooling-air pressure drop based on the exit rather than the commonly used entrance density. The use of exit density was further rationalized theoretically.

2. A sea-level correlation on the basis of entrance density gave fairly accurate results up to an altitude of 20,000 feet. For higher altitudes, however, the use of exit density wherever possible is recommended inasmuch as the error resulting from the use of entrance density increased at a rapidly increasing rate with altitude.

3. For an illustrative set of constant engine operating conditions, the errors involved in predictions made from the low-altitude correlation based on entrance rather than exit density were:

(a) Average head temperatures of 9°, 13°, and 36° F for a constant cooling-air pressure drop of 10 inches of water at 20,000, 30,000, and 50,000 feet, respectively.

(b) Cooling-air pressure drops of 1, 2, and 14 inches of water for an average head temperature of 400° F at 20,000, 30,000, and 50,000 feet, respectively.

AIRCRAFT ENGINE RESEARCH LABORATORY,
NATIONAL ADVISORY COMMITTEE FOR AERONAUTICS,
CLEVELAND, OHIO, *May 9, 1946.*

APPENDIX A

SYMBOLS

The following symbols are used in this report:

A outside-wall area of cylinder head, sq in.
c_p specific heat of air, 0.24 Btu/(lb)(° F)
F cylinder friction factor
F_1 cylinder friction factor at $\sigma_{en}\Delta p=1$ in. water
F/A fuel-air ratio of engine charge
f cylinder free-flow area ratio
g acceleration due to gravity, 32.2 ft/sec^2
h heat-transfer coefficient from outside wall of cylinder head to cooling air, Btu/(sq in.) (° F) (sec)
J mechanical equivalent of heat, 778 ft-lb/Btu
N engine speed, rpm
p absolute pressure of cooling air, in. Hg
p_e engine absolute exhaust pressure, in. Hg
Δp cooling-air pressure drop across engine, in. water
Δp_f cooling-air pressure drop due to skin friction within cylinder interfin passages, in. water
Δp_m cooling-air pressure drop due to momentum change of cooling air across cylinder, in. water
T_a cooling-air temperature ahead of engine, ° F
T_b cylinder-barrel temperature, ° F
T_c carburetor inlet-air temperature, ° F
T_g mean effective gas temperature, ° F
$T_{g,80}$ mean effective gas temperature corrected to dry inlet-manifold temperature of 80° F, ° F
T_h cylinder-head temperature, ° F
T_m dry inlet-manifold temperature, ° F
T_r cooling-air temperature at rear of engine, ° F
ΔT cooling-air temperature rise across engine, ° F
U tip speed of engine-stage blower, ft/sec
V cooling-air velocity within interfin passages, ft/sec
W_a engine cooling-air weight flow, lb/sec
W_c engine charge-air weight flow, lb/sec
ρ cooling-air density, lb/cu ft
σ density of cooling air relative to standard air density of 0.0765 lb/cu ft, $\rho/0.0765$

Subscripts:

av average condition between entrance and exit
en at cylinder entrance
ex at cylinder exit

Correlation constants:

$K, K_1, K_2, K_3, K_4, K_5, K_6, k, k_1, k_2, k_3, k_4, k_5$

Correlation exponents:

$b, m, n, r, r', s, x, y, Z$

APPENDIX B

THEORETICAL DERIVATION OF EFFECT OF COOLING-AIR-DENSITY CHANGE ON ENGINE COOLING

An expression will be derived for the cooling-correlation equation in which account is taken of the effect on the cooling-air pressure drop of the change in cooling-air density from the front to the rear of the cylinder. From this expression and the experimental data at low altitude (5000 ft), an equation is obtained by means of which the cooling of the engine at any altitude may be predicted.

In the derivation of the expression for the cooling-air pressure drop, simplifications are made that have been found to introduce a small inaccuracy.

Simplified pressure-drop equation.—With reference to figure 18, the pressure losses across an engine cylinder can be divided and expressed as follows: Entrance loss (station 0 to station 1)

$$\Delta p_{en}=\frac{1}{5.2g}\frac{\rho_{en}V_{en}^2}{2}(1-f^2) \tag{11}$$

Skin-friction losses within the cylinder interfin passages, (station 1 to station 2)

$$\Delta p_f=\frac{F}{5.2g}\frac{\rho_{av}V_{av}^2}{2}$$

or, based on the entrance conditions and exit-entrance density ratio (σ_{av} is taken as the arithmetic average of σ_{en} and σ_{ex})

$$\Delta p_f=\frac{1}{5.2g}\frac{\rho_{en}V_{en}^2}{2}\left(\frac{2F}{1+\frac{\sigma_{ex}}{\sigma_{en}}}\right) \tag{12}$$

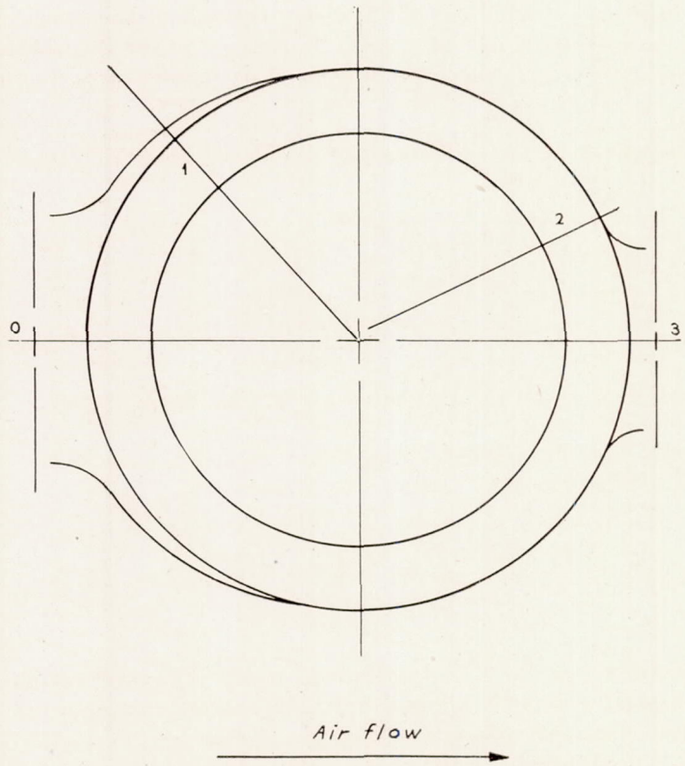

FIGURE 18.—Diagram of cooling-air flow path across engine cylinder.

Momentum loss (station 1 to station 2)

$$\Delta p_m=\frac{\rho_{en}V_{en}}{5.2g}(V_{ex}-V_{en})$$

or

$$\Delta p_m=\frac{1}{5.2g}\frac{\rho_{en}V_{en}^2}{2}\left[2\left(\frac{1}{\frac{\sigma_{ex}}{\sigma_{en}}}-1\right)\right] \tag{13}$$

Exit-pressure recovery (station 2 to station 3)

$$\Delta p_{ex}=\frac{\rho_{ex}V_{ex}f}{5.2g}(fV_{ex}-V_{ex})$$

or

$$\Delta p_{ex}=\frac{1}{5.2g}\frac{\rho_{en}V_{en}^2}{2}\left[\frac{2(f^2-f)}{\frac{\sigma_{ex}}{\sigma_{en}}}\right] \tag{14}$$

The total-pressure loss across an engine cylinder is given by the summation of the component losses as

$$\Delta p=\frac{1}{5.2g}\frac{\rho_{en}V_{en}^2}{2}\left[(1-f^2)+\frac{2F}{1+\frac{\sigma_{ex}}{\sigma_{en}}}+2\left(\frac{1}{\frac{\sigma_{ex}}{\sigma_{en}}}-1\right)+\frac{2(f^2-f)}{\frac{\sigma_{ex}}{\sigma_{en}}}\right] \tag{15}$$

Comparison between the values of pressure drop computed from equation (15) and from the more rigorous methods of reference 5 indicated a maximum difference of 10 percent for extreme conditions with respect to present cylinder and operating conditions.

Cooling-correlation equation including compressibility effect.—The simplified pressure-drop equation when solved for W_a, which is proportional to $\rho_{en}V_{en}$, can be written as

$$W_a=\frac{k_1(\sigma_{en}\Delta p)^{1/2}}{\left[(1-f^2)+\frac{2F}{1+\frac{\sigma_{ex}}{\sigma_{en}}}+2\left(\frac{1}{\frac{\sigma_{ex}}{\sigma_{en}}}-1\right)+\frac{2(f^2-f)}{\frac{\sigma_{ex}}{\sigma_{en}}}\right]^{1/2}} \tag{16}$$

Substitution in the basic cooling-correlation equation (equation (1)) results in

$$\frac{\frac{T_h-T_a}{T_g-T_h}}{W_c^n}=\frac{K_1\left[(1-f^2)+\frac{2F}{1+\frac{\sigma_{ex}}{\sigma_{en}}}+2\left(\frac{1}{\frac{\sigma_{ex}}{\sigma_{en}}}-1\right)+\frac{2(f^2-f)}{\frac{\sigma_{ex}}{\sigma_{en}}}\right]^{r/2}}{k(\sigma_{en}\Delta p)^{r/2}} \tag{17}$$

Multiplying both sides of equation (17) by $(\sigma_{en}\Delta p)^m$ gives

$$\frac{T_h-T_a}{T_g-T_h}\frac{(\sigma_{en}\Delta p)^m}{W_c^n}=$$

$$\frac{K_1\left[(1-f^2)+\frac{2F}{1+\frac{\sigma_{ex}}{\sigma_{en}}}+2\left(\frac{1}{\frac{\sigma_{ex}}{\sigma_{en}}}-1\right)+\frac{2(f^2-f)}{\frac{\sigma_{ex}}{\sigma_{en}}}\right]^{r/2}}{k(\sigma_{en}\Delta p)^{r/2-m}} \tag{18}$$

The friction factor F is proportional to the 0.2 power of the cooling-air Reynolds number for turbulent flow through the cylinder interfin passages. Because of this small variation of F with Reynolds number, the following simplifications in the determination of an expression for F are permissible:

(a) The viscosity in the Reynolds number parameter is assumed constant.

(b) The mass flow in the Reynolds number parameter is taken as proportional to $(\sigma_{en}\Delta p)^{1/2}$.

With these simplifications F can be written:

$$F=F_1(\sigma_{en}\Delta p)^{0.1} \tag{19}$$

where F_1 is the value of F at $\sigma_{en}\Delta p$ equal to 1 inch of water.

Combination of equations (18) and (19) gives

$$\frac{T_h-T_a}{T_g-T_h}\frac{(\sigma_{en}\Delta p)^m}{W_c^n}=$$

$$\frac{K_1}{k}\left[\frac{(1-f^2)+\frac{2F_1(\sigma_{en}\Delta p)^{0.1}}{1+\frac{\sigma_{ex}}{\sigma_{en}}}+2\left(\frac{1}{\frac{\sigma_{ex}}{\sigma_{en}}}-1\right)+\frac{2(f^2-f)}{\frac{\sigma_{ex}}{\sigma_{en}}}}{(\sigma_{en}\Delta p)^{1-\frac{2m}{r}}}\right]^{r/2} \tag{20}$$

The left-hand side of equation (20) when equated to a constant is recognized as the usual form of the NACA correlation relation (equation 2(a)); the right-hand side introduces the effect of change in σ_{ex}/σ_{en}. The constants K_1/k, F_1, f, m, and r in equation (20) will be evaluated from the known air-flow characteristics of the engine cylinder and from the low-altitude experimental data (5000 ft) at which condition the value of σ_{ex}/σ_{en} was found to be effectively constant at 0.83 for a wide range of operating conditions. When the values of these constants are inserted in equation (20), this equation may be used to predict the cooling at other values of σ_{ex}/σ_{en} corresponding to any altitude and operation.

Evaluation of constants of equation (20).—

(a) The friction factor F_1 is determined as 0.9 from air-flow and pressure-loss data obtained at sea level in single-cylinder experiments on an R–2800–21 engine.

(b) The value of free-flow area ratio f is taken as 0.1 as estimated from measurements on an R–2800–21 engine. An accurate value of f is not required as the terms involving f are small compared with the other terms in the numerator of the right-hand side of equation (20).

(c) The values of K_1/k and r are determined from the cooling data obtained for σ_{ex}/σ_{en} equal to 0.83 (5000-ft altitude investigation) in the following manner:

For σ_{ex}/σ_{en} equal to 0.83, equation (20) must reduce to equation (7). Thus,

$$\frac{K_1}{k}\left[\frac{(1-f^2)+\frac{2F_1(\sigma_{en}\Delta p)^{0.1}}{1+0.83}+2\left(\frac{1}{0.83}-1\right)+\frac{2(f^2-f)}{0.83}}{(\sigma_{en}\Delta p)^{1-\frac{2m}{r}}}\right]^{r/2}=0.42 \tag{21}$$

On substitution of the numerical values of F_1 and f, and rearrangement, equation (21) becomes

$$1.184+0.984(\sigma_{en}\Delta p)^{0.1}=\left(0.42\frac{k}{K_1}\right)^{2/r}(\sigma_{en}\Delta p)^{1-\frac{2m}{r}} \tag{22}$$

When the left-hand side of equation (22) is plotted against $\sigma_{en}\Delta p$ on logarithmic coordinate paper, the slope equals the

exponent $1-\frac{2m}{r}$. Figure 19 presents this plot and indicates a value of $1-\frac{2m}{r}$ of -0.04. The value of r, as calculated from this equality and the experimental value of m (indicated by equation (7) as equal to 0.35), is found to be 0.67. The ordinate in figure 19 at $\sigma_{en}\Delta p$ equal to 1 inch of water gives the value of $\left(0.42\frac{k}{K_1}\right)^{2/r}$ as 2.2 from which $\frac{K_1}{k}$ is calculated

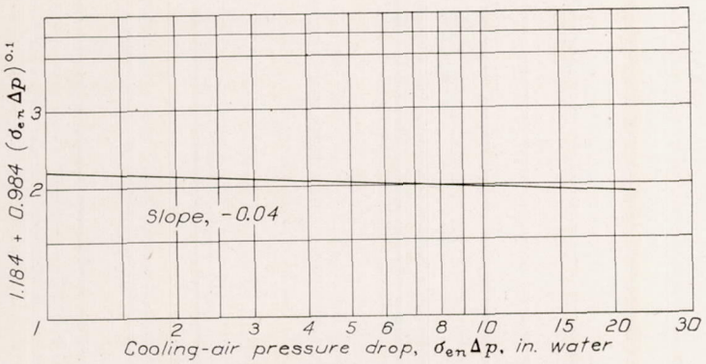

FIGURE 19.—Plot for evaluation of parameters r and $\frac{K_1}{k}$ of equation (22).

to be 0.32. When the foregoing values are substituted for the constants and exponents, equation (20) becomes

$$\frac{T_h-T_a}{T_g-T_h}\frac{(\sigma_{en}\Delta p)^{0.35}}{W_c^{0.60}}=$$

$$0.32\left[\frac{0.99+\frac{1.8(\sigma_{en}\Delta p)^{0.1}}{1+\frac{\sigma_{ex}}{\sigma_{en}}}+2\left(\frac{1}{\frac{\sigma_{ex}}{\sigma_{en}}}-1\right)+\frac{-0.18}{\frac{\sigma_{ex}}{\sigma_{en}}}}{(\sigma_{en}\Delta p)^{-0.04}}\right]^{50.335} \tag{23}$$

The value of $n=0.60$ is obtained from the experimental data at 5000-foot altitude. The quantity $\frac{T_h-T_a}{T_g-T_h}\frac{(\sigma_{en}\Delta p)^{0.35}}{W_c^{0.60}}$ is computed from equation (23), which was established from the theoretical analysis and the cooling data at σ_{ex}/σ_{en} equal to 0.83, and is plotted as dashed lines in figure 10 against σ_{ex}/σ_{en} for two extreme values of $\sigma_{en}\Delta p$ (0.5 and 20 in. water). It is noted that $\sigma_{en}\Delta p$ introduces negligible spread in the curves, which indicates that $\sigma_{en}\Delta p$ is of small significance in the right-hand side of equation (23) or its generalized form (equation (20)), and hence, that equation (23) can be approximated by equation (2).

APPENDIX C

JUSTIFICATION FOR USE OF INLET COOLING-AIR TEMPERATURE IN CORRELATION EQUATIONS

The following derivation is presented to show the validity of the use in the correlation equations (for example, equation (1)) of the inlet cooling-air temperature instead of the local cooling-air temperature in the vicinity of the location at which the cylinder temperature is measured.

If the cylinder temperature at the rear of the head is under investigation, then, on the basis of local cooling-air temperature, the correlation equation (1) would be written

$$\frac{\frac{T_h-T_r}{T_g-T_h}}{W_c^n}=\frac{K_5}{W_a^{r'}} \tag{24}$$

where the exponent r' differs numerically from the exponent r in equation (1).

From equations (28) and (29) developed in appendix D,

$$T_r-T_a=\Delta T=\frac{k_2AW_a^{(x-1)}(T_h-T_a)}{c_p} \tag{25}$$

When T_r is eliminated from equation (24) by means of equation (25), there results

$$\frac{T_h-T_a-\frac{k_2AW_a^{(x-1)}(T_h-T_a)}{c_p}}{(T_g-T_h)W_c^n}=\frac{K_5}{W_a^{r'}} \tag{26}$$

Rearrangement of terms gives

$$\frac{\frac{T_h-T_a}{T_g-T_h}}{W_c^n}=\frac{K_5}{W_a^{r'}\left[1-\frac{k_2AW_a^{(x-1)}}{c_p}\right]} \tag{27}$$

For a given engine installation, the right-hand side of equation (27) is a function only of W_a and can be approximated within the limits of the variation of W_a of interest in engine cooling by K_1/W_a^r. Equation (27) then becomes

$$\frac{\frac{T_h-T_a}{T_g-T_h}}{W_c^n}=\frac{K_1}{W_a^r} \tag{28}$$

which is the same as equation (1) and similar in form to equation (24). Thus, use of the inlet cooling-air temperature instead of the local cooling-air temperature merely results in a change of the constant and cooling-air exponent in the correlation equation.

If the assumption is made that the temperature rise of the cooling air to any given location around the cylinder as a precentage of the total temperature rise is constant for all operating conditions, then the same transformation from local-air temperature to inlet-air temperature as shown by equations (24) to (28) can be made for any local cylinder temperature.

APPENDIX D

ENGINE COOLING-AIR TEMPERATURE-RISE EQUATION

For convenience in cooling predictions, the engine cooling-air temperature rise is related to the other known cooling variables by equating the heat absorbed by the cooling air to the heat transferred from the cylinder walls to the cooling air. Thus,

$$W_a c_p \Delta T = hA(T_h - T_a) \tag{28}$$

Because

$$h = k_2(W_a)^x \tag{29}$$

and

$$W_a = k_3(\sigma_{ex}\Delta p)^y \tag{30}$$

the solution for $\frac{\Delta T}{T_h - T_a}$ can be made in terms of $\sigma_{ex}\Delta p$,

$$\frac{\Delta T}{T_h - T_a} = k_4(\sigma_{ex}\Delta p)^{y(x-1)} \tag{31}$$

The value of the exponent $y(x-1)$ is found from the data to be -0.16 for the cylinder heads and -0.095 for the barrels. Because of the low values of this exponent, satisfactory correlation of $\frac{\Delta T}{T_h - T_a}$ with $\sigma_{en}\Delta p$ should also be obtainable; the use of $\sigma_{en}\Delta p$ rather than $\sigma_{ex}\Delta p$ is preferred in the $\frac{\Delta T}{T_h - T_a}$ relation because the results can then, in some applications, be more directly used with the correlation equation at little sacrifice in accuracy. Thus, for all practical purposes

$$\frac{\Delta T}{T_h - T_a} = k_5(\sigma_{en}\Delta p)^z \tag{32}$$

Plots of $\frac{\Delta T}{T_h - T_a}$ and $\frac{\Delta T}{T_b - T_a}$ against $\sigma_{en}\Delta p$ made from the cooling measurements are presented in figure 20 for the engine heads and barrels. The use of figure 20 to make altitude engine-cooling predictions is illustrated in appendix E.

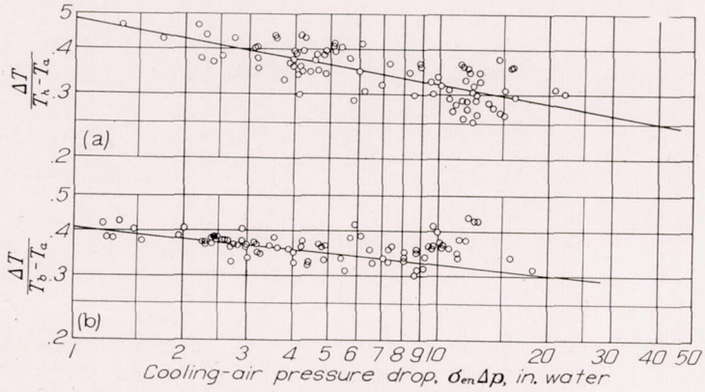

(a) Slope, −0.18; engine heads.
(b) Slope, −0.10; engine barrels.

FIGURE 20.—Variation in cooling-air temperature-rise parameter with cooling-air pressure drop $\sigma_{en}\Delta p$ for engine heads and barrels.

APPENDIX E

HIGH-ALTITUDE ENGINE-COOLING PREDICTION

The use of $\sigma_{ex}\Delta p$ in the cooling-correlation equation, as required for accurately predicting cooling at altitude, introduces the problem of evaluating σ_{ex}. This problem is complicated by the fact that σ_{ex} is not directly obtainable from the atmospheric pressure and temperature values (including the corrections due to ram) as is the case with σ_{en} but further involves the engine heat rejection and cooling-air pressure drop. For this reason, simultaneous solution for σ_{ex} and of the correlation equation is required; as direct solution is difficult, the method of successive approximations is used.

The correlation relations that must be established in the low-altitude or sea-level engine-cooling experiments for subsequent use in the determination of the cooling obtained at the high altitudes are, for the purpose of review, tabulated as follows:

1. The correlation equation (equation (4)) graphically represented for the subject experiments by the correlation line of figure 11
2. The $T_{g,80}$ relation described by the curves of figure 6
3. The cooling-air temperature-rise equation (equation (32)) graphically represented in figure 20

The quantity σ_{ex}/σ_{en} is given by the general gas law

$$\sigma_{ex}/\sigma_{en} = \frac{p_{ex}}{p_{en}} \frac{T_a + 460}{T_r + 460} = \frac{1 - \frac{\Delta p}{p_{en}}}{1 + \frac{\Delta T}{T_a + 460}} \tag{33}$$

The quantity σ_{en} is calculated from the entrance cooling-air pressure and temperature. The quantity σ_{ex} can be computed from σ_{en} by means of equation (33).

For the purpose of illustrating the method of obtaining simultaneous solution of the foregoing pertinent relations to determine the cooling obtained at altitude, two typical problems are herein assumed and solved in step-by-step fashion.

Calculation of cooling-air pressure-drop requirements at altitude, case 1.—

The following operating conditions are assumed:

1. Engine charge-air consumption, lb/sec	3.5
2. Fuel-air ratio of charge	0.100
3. Dry inlet-manifold temperature, ° F	250
4. Engine exhaust pressure, in. Hg absolute	30
5. Altitude of operation, ft	35,000

for which, including ram corrections,

$$T_a = 6° \text{ F}$$

$$p_{en} = 8.46 \text{ inches mercury absolute}$$

The cooling-air pressure drop Δp for satisfying the cooling requirement for an average rear-middle head temperature (T_{19} in fig. 4) of 400° F must be found.

6. From figure 6 for items 2 and 4,

$$T_{g,80} = 1000° \text{ F}$$

7. Correction of $T_{g,80}$ to a dry inlet-manifold temperature of 250° F gives

$$T_g=1000+0.8\ (250-80)=1136°\ \text{F}$$

8. From items 5 and 7 for $T_h=400°$ F,

$$\frac{T_h-T_a}{T_g-T_h}=\frac{400-6}{1136-400}=0.535$$

9. From items 1 and 8,

$$\frac{\dfrac{T_h-T_a}{T_g-T_h}}{W_c^{0.60}}=\frac{0.535}{3.50^{0.60}}=0.252$$

10. From item 9 and equation (9) (or fig. 11),

$$\sigma_{ex}\Delta p=3.5 \text{ inches water}$$

Solution for σ_{ex} is now required and involves the method of successive approximation.

As for the first approximation, assume

$$\sigma_{en}=\sigma_{ex}$$

11. Solution for σ_{en} from item 5 and the standard sea-level air conditions of a pressure of 29.92 inches of mercury absolute and a temperature of 519° R gives

$$\sigma_{en}=\frac{8.46}{29.92}\times\frac{519}{466}=0.315$$

12. From items 10 and 11, the first approximation value of Δp is

$$\Delta p=\frac{3.5}{0.315}=11.1 \text{ inches water}$$

13. For $\sigma_{en}\Delta p=\sigma_{ex}\Delta p=3.5$ inches water (assumption in first approximation solution), figure 20 gives

$$\frac{\Delta T}{T_h-T_a}=0.386$$

14. Thus, from item 5 ($T_a=6°$ F) for $T_h=400°$ F,

$$\Delta T=0.386\times394=152°\ \text{F}$$

15. From equation (33) and items 5, 12, and 14,

$$\frac{\sigma_{ex}}{\sigma_{en}}=\frac{1-\dfrac{11.1}{13.6\times8.46}}{1+\dfrac{152}{466}}=\frac{0.904}{1.326}=0.682$$

which is the second approximation value of σ_{ex}/σ_{en}.

16. As the second approximation for Δp, from items 10, 11, and 15,

$$\Delta p=\frac{3.5}{0.315\times0.682}=16.3 \text{ inches water}$$

17. From items 11 and 16,

$$\sigma_{en}\Delta p=0.315\times16.3=5.14 \text{ inches water}$$

18. From figure 20 for item 17,

$$\frac{\Delta T}{T_h-T_a}=0.36$$

19. Thus, from item 5 for $T_h=400°$ F,

$$\Delta T=0.36\times394=142°\ \text{F}$$

20. From equation (33) and items 5, 16, and 19,

$$\frac{\sigma_{ex}}{\sigma_{en}}=\frac{1-\dfrac{16.3}{13.6\times8.46}}{1+\dfrac{142}{466}}=\frac{0.858}{1.305}=0.658$$

which is the third approximation value of σ_{ex}/σ_{en}. Thus, as the third approximation for Δp

$$\Delta p=\frac{3.5}{0.315\times0.658}=16.9 \text{ inches water}$$

Recalculation for σ_{ex}/σ_{en} gives a value of 0.654 as compared with 0.658 obtained in the third approximation. The value of σ_{ex}/σ_{en} converges very rapidly and a third approximation for σ_{ex}/σ_{en}, and thus for Δp, is sufficient.

The pressure-drop value of 16.9 inches of water obtained in the foregoing calculations compares with 13.6 inches of water, which would be given by the correlation based on $\sigma_{en}\Delta p$ (equation (7)).

Calculation of average head temperature obtained at altitude, case 2.—For the conditions given in items 1 through 5, a cooling-air pressure drop of 10 inches of water is assumed to be available for which it is desired to calculate the resulting head temperature.

21. From item 11 and for $\Delta p=10$ inches water,

$$\sigma_{en}\Delta p=3.15 \text{ inches water}$$

22. From figure 20 and item 21,

$$\frac{\Delta T}{T_h-T_a}=0.39$$

23. As a first approximation, assume $T_h=400°$ F. Then, from items 5 ($T_a=6°$ F) and 22,

$$\Delta T=0.39\times394=154°\ \text{F}$$

24. From items 5, 23, and equation (33),

$$\frac{\sigma_{ex}}{\sigma_{en}}=\frac{1-\dfrac{10}{13.6\times8.46}}{1+\dfrac{154}{466}}=\frac{0.913}{1.33}=0.686$$

25. From items 11 and 24 and for $\Delta p=10$ inches water,

$$\sigma_{ex}\Delta p=0.315\times0.686\times10=2.16 \text{ inches water}$$

26. From equation (9) (or fig. 11) and item 25,

$$\frac{\dfrac{T_h-T_a}{T_g-T_h}}{W_c^{0.60}}=0.298$$

27. From items 1, 5, 7, and 26,

$$T_h = 442° \text{ F}$$

28. As the second approximation, let

$$T_h = 442° \text{ F}$$

Then, from items 5 and 22,

$$\Delta T = 0.39 \times 436 = 170° \text{ F}$$

29. From items 5 and 28 and equation (33),

$$\frac{\sigma_{ex}}{\sigma_{en}} = \frac{1 - \frac{10}{13.6 \times 8.46}}{1 + \frac{170}{466}} = \frac{0.913}{1.365} = 0.668$$

30. From items 11 and 29 and for $\Delta p = 10$ inches water,

$$\sigma_{ex} \Delta p = 0.315 \times 0.668 \times 10 = 2.10 \text{ inches water}$$

31. From equation (9) (or fig. 11) and item 30,

$$\frac{T_h - T_a}{\frac{T_g - T_h}{W_c^{0.60}}} = 0.301$$

32. From items 1, 5, 7, and 31,

$$T_h = 446° \text{ F}$$

which checks very closely with the second approximation value and is therefore the required value.

The derived T_h value of 446° F compares with 428° F, which would be obtained from the correlation based on $\sigma_{en} \Delta p$ (equation (7)).

REFERENCES

1. Pinkel, Benjamin: Heat-Transfer Processes in Air-Cooled Engine Cylinders. NACA Rep. No. 612, 1938.
2. Pinkel, Benjamin, and Rubert, Kennedy F.: Correlation of Wright Aeronautical Corporation Cooling Data on the R–3350–14 Intermediate Engine and Comparison with Data from the Langley 16-Foot High-Speed Tunnel. NACA ACR No. E5A18, 1945.
3. Corson, Blake W., Jr., and McLellan, Charles H.: Cooling Characteristics of a Pratt & Whitney R–2800 Engine Installed in a NACA Short-Nose High-Inlet-Velocity Cowling. NACA ACR No. L4F06, 1944.
4. Becker, John V., and Baals, Donald D.: Analysis of Heat and Compressibility Effects in Internal Flow Systems and High-Speed Tests of a Ram-Jet System. NACA Rep. No. 773, 1943.
5. Williams, David T.: High-Altitude Cooling. II—Air-Cooled Engines. NACA ARR No. L4I11a, 1944.
6. Neustein, Joseph, and Schafer, Louis J., Jr.: Comparison of Several Methods of Predicting the Pressure Loss at Altitude across a Baffled Aircraft-Engine Cylinder. NACA Rep. No. 858, 1946.
7. Richards, William M. S., and Erdman, Frank H.: Prediction of Engine Cooling Requirements. SAE Jour. (Trans.), vol. 53, no. 7, July 1945, pp. 410–419.
8. Ellerbrock, Herman H., Jr., and Rollin, Vern G.: Correlation of Single-Cylinder Cooling Tests of a Pratt & Whitney R–2800–21 Engine Cylinder with Wind-Tunnel Tests of a Pratt & Whitney R–2800–27 Engine. NACA ARR No. 3L14, 1943.

TABLE I—SUMMARY OF FLIGHT CONDITIONS

Altitude (ft)	Engine power (bhp)	Pressure drop (in. water)	Engine speed (rpm)
5,000	800	Variable	2550
5,000	1000	do	2550
5,000	1300	do	2550
5,000	1500	do	2550
5,000	800	Constant	Variable
5,000	Variable	do	2550
5,000	1100	Variable	2550
5,000	Variable	Constant	2550
5,000	1000	do	Variable
5,000	Variable	Variable	2550
7,000	2000	do	2700
10,000	1500	do	2550
10,000	1000	do	Variable
15,000	1100	do	do
25,000	1000	do	2550
25,000	1100	do	2550
25,000	1000	do	2550
25,000	1500	do	2550
25,000	1800	do	2700
25,000	Variable	Constant	2550
25,000	1000	Variable	2550
25,000	Variable	do	2550
25,000	do	Constant	Variable
30,000	1300	Variable	2550
30,000	1500	do	2550
30,000	1100	do	2550
30,000	Variable	Constant	2600
35,000	1200	Variable	2550
35,000	1200	do	2550

U. S. GOVERNMENT PRINTING OFFICE: 1949

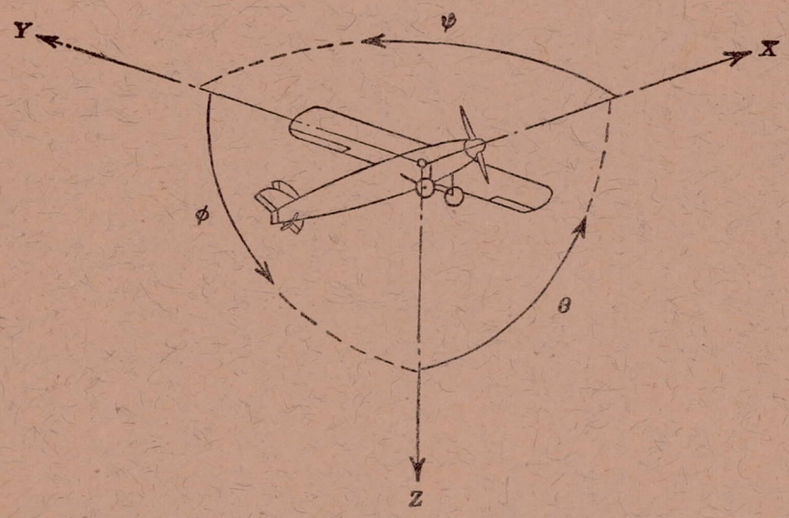

Positive directions of axes and angles (forces and moments) are shown by arrows

Axis		Force (parallel to axis) symbol	Moment about axis			Angle		Velocities	
Designation	Symbol		Designation	Symbol	Positive direction	Designation	Symbol	Linear (component along axis)	Angular
Longitudinal	X	X	Rolling	L	$Y \longrightarrow Z$	Roll	ϕ	u	p
Lateral	Y	Y	Pitching	M	$Z \longrightarrow X$	Pitch	θ	v	q
Normal	Z	Z	Yawing	N	$X \longrightarrow Y$	Yaw	ψ	w	r

Absolute coefficients of moment

$C_l = \frac{L}{qbS}$ (rolling) $\quad C_m = \frac{M}{qcS}$ (pitching) $\quad C_n = \frac{N}{qbS}$ (yawing)

Angle of set of control surface (relative to neutral position), δ. (Indicate surface by proper subscript.)

4. PROPELLER SYMBOLS

D Diameter
p Geometric pitch
p/D Pitch ratio
V' Inflow velocity
V_s Slipstream velocity
T Thrust, absolute coefficient $C_T = \frac{T}{\rho n^2 D^4}$
Q Torque, absolute coefficient $C_Q = \frac{Q}{\rho n^2 D^5}$
P Power, absolute coefficient $C_P = \frac{P}{\rho n^3 D^5}$
C_s Speed-power coefficient $= \sqrt[5]{\frac{\rho V^5}{P n^2}}$
η Efficiency
n Revolutions per second, rps
Φ Effective helix angle $= \tan^{-1}\left(\frac{V}{2\pi r n}\right)$

5. NUMERICAL RELATIONS

1 hp=76.04 kg-m/s=550 ft-lb/sec
1 metric horsepower=0.9863 hp
1 mph=0.4470 mps
1 mps=2.2369 mph

1 lb=0.4536 kg
1 kg=2.2046 lb
1 mi=1,609.35 m=5,280 ft
1 m=3.2808 ft